

## Stochastic simulations of the quantum Zeno effect

W. L. Power and P. L. Knight

*Optics Section, Blackett Laboratory, Imperial College, London SW7 2BZ, England*

(Received 19 June 1995)

We perform stochastic simulations of the quantum Zeno effect experiment of the type realized with trapped cooled ions. The results are carefully examined for the case where the experiment is performed on a single atomic particle. The results of the simulations for a single ion exhibit the probabilistic behavior that is required to satisfy the collapse of the wave-packet hypothesis. When a large ensemble of ions is described by the simulations, the results are the same as those produced using the density-matrix method. In this way the stochastic simulation methods provide a link between these two approaches, as they are compatible with each in the appropriate regime. The results are also discussed in terms of what may be observed experimentally given the practical limitations of performing experiments with individual ions.

PACS number(s): 42.50.Ct, 42.50.Lc

### I. INTRODUCTION

The nature of the measurement process has been one of the most fundamental problems in quantum mechanics since it was first introduced. One of the most surprising features of measurements in quantum mechanics is that the act of measurement changes the state of the system that has been observed. Misra and Sudarshan [1] pointed out that an unstable quantum system could be prevented from decaying by continuously observing its undecayed state. Coherent unitary time evolution leads to a transition probability proportional to the square of the elapsed time (for short times). Repeated observation of the state of excitation by a sequence of measurements separated by a time interval such that evolution between measurements is within this quadratic time-dependence regime leads to a “freezing” or inhibition of the transition. If the time evolution is in fact an irreversible decay described by a Fermi “golden rule” rate, then the transition probability at short times is *linearly* proportional to the elapsed time and a measurement sequence will not lead to the inhibition of decay. Attempts were made to observe this effect by looking for the inhibition of decay of unstable particles that were repeatedly observed in, for example, bubble-chamber tracks. However, no clear evidence of this type has been found. The reason for this lack of success of course derives from our inability to make repeated measurements within the correlation time of the decay process: only at such very short times does a decay depend quadratically on time in the requisite manner.

Many other forms of this so-called quantum Zeno effect have been proposed [2–5]. In particular, Cook [6] suggested a dynamical version of this effect in which a coherently driven atomic transition (in other words, a unitary evolution rather than a decay) would be inhibited by repeated measurements. Itano *et al.* [7] performed such an experiment using several thousand trapped ions. The ions were slowly driven between two energy levels using an rf source, and the proportion of ions in each state was probed at regular intervals using a laser. Quantitative predictions of the numbers of ions found in each state were made using the assumption that the measurement of the state of the ions by the laser acted to

reduce the wave packet by converting the state of the ions from a superposition state to a statistical mixture of ions in each of the two energy levels. It was subsequently pointed out by Frerichs and Schenzle [8], and by Block and Berman [9] that the results of the experiment could equally well be described using a density-matrix analysis of the atomic system that included the energy levels used to perform the measurement. In their analysis it was no longer necessary to make an assumption about the collapse of the wave packet, and so they argued that the experiment could no longer be viewed as a demonstration of this effect.

It has recently been proposed that the quantum Zeno effect experiment be repeated using only a single trapped ion, and preparations for such an experiment are underway [10]. In this case the density-matrix analysis is no longer directly relevant as it stands, as it assumes that the experiment is performed on a large number of ions simultaneously. The fluorescent signal is proportional to the populations predicted from the density matrix only when a reasonably large number of independent sources are contributing to the signal. Nevertheless, the density matrix determines the statistics and the probabilities for particular realizations through, for example, the waiting time distributions of the fluorescent emissions, although without the direct clarity of the newer stochastic methods. For an ensemble of ions undergoing repeated measurement, all we require for inhibition is the destruction of coherence by the repeated coupling to a broad decaying state, so that the superposition state coherence is destroyed. Such an ensemble-averaged relaxation of the coherence can be understood without recourse to state reduction ideas [11]. To examine the behavior of the experiment for the case of a single atomic particle in a more direct way, we can apply newly developed simulation techniques [12–19], which describe how acquisition of knowledge about the single ion is used to condition the state describing that realization. The various methods for performing stochastic simulations describe quantum trajectories for the states of the system, and are determined by random processes. To generate the ensemble results, the stochastic simulation is repeated several times and an average result calculated. One advantage of these new stochastic methods is that we may examine

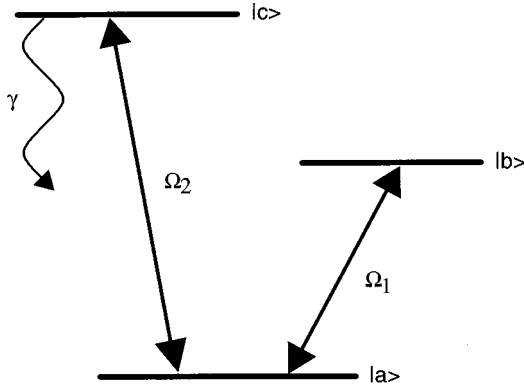


FIG. 1. The three-level  $v$  configuration considered by Itano *et al.* The radio-frequency transition between levels  $|a\rangle$  and  $|b\rangle$  is slowly driven with a Rabi frequency  $\Omega_1$ . During the measurement pulses the optical transition between  $|a\rangle$  and  $|c\rangle$  is driven with a Rabi frequency  $\Omega_2$ ; the rate of spontaneous emission from  $|c\rangle$  is  $\gamma$ .

the behavior of individual trajectories and infer some of the behavior of individual particles.

## II. QUANTUM ZENO EFFECT

The energy-level system used for the quantum Zeno effect, as proposed by Cook [6] and realized by Itano *et al.* [7], is a three-level  $v$  configuration of the kind shown in Fig. 1. The transition from  $|a\rangle$  to  $|b\rangle$  is in the radio-frequency regime, and the rate of spontaneous emission from  $|b\rangle$  is very small and can safely be neglected. In the absence of any measurement, a  $\pi$  pulse applied to this transition would transfer an atom initially in the ground state entirely into the excited state. If the pulse were allowed to continue longer, the atom would undergo Rabi oscillations between the two states with frequency  $\Omega_1$ . To observe the populations of the two levels, the system is coupled by a strong optical transition (with Rabi frequency  $\Omega_2$ ) to the level  $|c\rangle$ , and measurements are made by observing the scattered fluorescence from the transition between  $|a\rangle$  and  $|c\rangle$  when the atom is illuminated by regular pulses of resonant laser light, as shown in Fig. 2 (rectangular pulses have been used in the theoretical analysis, although in the experiment there is a short time period during which the pulse is switched on and off). The time scales for this transition are such that  $\gamma, \Omega_2 \gg \Omega_1$ , where  $\gamma$  is the spontaneous decay rate of population from level  $|c\rangle$  to  $|a\rangle$ . According to the projection postulate [11], each measurement pulse reduces the atomic density matrix to its diagonal elements. If this assumption is made, it is found that the population of level  $|b\rangle$ , if there have been  $n$  measurement pulses during a single rf  $\pi$  pulse, is given by [7]

$$P_b(T) = \frac{1}{2} [1 - \cos(\pi/n)^n]. \quad (1)$$

In practice this experiment was performed on approximately 5000  $\text{Be}^+$  ions stored in a Penning trap. At the end of each rf  $\pi$  pulse the proportion of ions in state  $|a\rangle$  was assumed to be proportional to the fluorescence from the  $|a\rangle$  to  $|c\rangle$  transition. The results were found to be in agreement with Eq. (1).

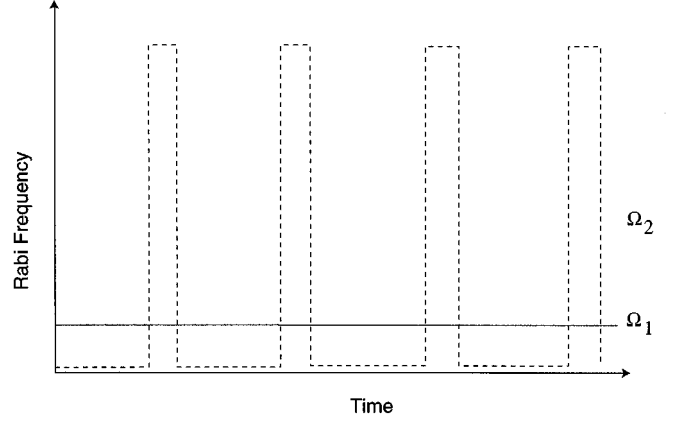


FIG. 2. The time dependence of the Rabi frequencies  $\Omega_1$  and  $\Omega_2$ .  $\Omega_1$  is constant and  $\Omega_2$  is normally zero, except during measurement pulses of length  $\tau$ , during which  $\Omega_2 \gg \Omega_1$ .

Frerichs and Schenzle [8] and Block and Berman [9] have independently argued that this agreement with the experimental results should not be taken as evidence for the collapse of the wave packet. They showed that the same results could be derived using density-matrix equations to describe the whole three-level system. After making the rotating-wave approximation, the density-matrix equations for the system are

$$\dot{\rho}_{cc} = -i\Omega_2(\rho_{ca} - \rho_{ac}^*) - \gamma\rho_{cc}, \quad (2)$$

$$\dot{\rho}_{ca} = -i\Omega_2(\rho_{aa} - \rho_{cc}) - i\Omega_1\rho_{cb} - \gamma\rho_{ca}, \quad (3)$$

$$\dot{\rho}_{bb} = -i\Omega_1(\rho_{ba} - \rho_{ba}^*), \quad (4)$$

$$\dot{\rho}_{ba} = i\Omega_1(\rho_{aa} - \rho_{bb}) - i\Omega_2\rho_{cb}^*, \quad (5)$$

$$\dot{\rho}_{aa} = -(\rho_{cc} + \rho_{bb}), \quad (6)$$

$$\dot{\rho}_{cb} = i\Omega_2\rho_{ba}^* - i\Omega_1\rho_{ca} - \frac{\gamma}{2}\rho_{cb}, \quad (7)$$

where  $\Omega_1$ ,  $\Omega_2$ , and  $\gamma$  are as defined above, and  $\rho_{ij}$  is the density-matrix element between levels  $|i\rangle$  and  $|j\rangle$ . These equations can be solved numerically [8,9] with the initial conditions  $\rho_{aa}(t=0)=1$ , all other  $\rho_{ij}(t=0)=0$ , and in Fig. 3 the population of state  $|b\rangle$  is shown as a function of time. For this plot there were five measurement pulses within a Rabi period, and each lasted for 0.02 of a Rabi period ( $2\pi/\Omega_1$ ). The measurement pulse field strength is  $\Omega_2 = \gamma = 250 * \Omega_1$ . The solutions to these equations show that the effect of the measurement laser is to destroy the coherence between levels  $|a\rangle$  and  $|b\rangle$ , after which only the diagonal elements of the density matrix remain [8]. The populations remaining after each pulse are consistent with both the experimental results and the collapse of the wave-packet predictions. The derivation of the density-matrix equations of motion contains many assumptions, but the collapse of the wave packet is never explicitly invoked.

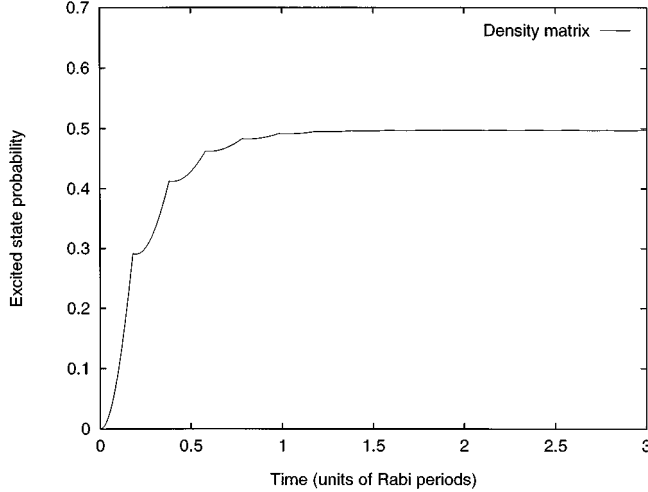


FIG. 3. The population of state  $|b\rangle$  as a function of time as calculated using the density-matrix method. The population is given by the element  $\rho_{bb}$  of the density matrix. The value of  $\Omega_1$  is  $2\pi$  and  $\Omega_2$  is  $250(2\pi)$ , as is  $\gamma$ . There are five measurement pulses within each Rabi cycle of the  $|a\rangle$  to  $|b\rangle$  transition, and each measurement pulse lasts for 0.02 of the Rabi period.

### III. STOCHASTIC METHODS

One of the major assumptions behind the density-matrix approach is that the experiment is described by the evolution of a large ensemble of independent systems. Of course, the density-matrix approach can be used to derive waiting time distributions and so on, which determine the dynamics of quantum systems of relevance to (say) quantum jumps. The basis of the quantum jump model as developed, for example, by Carmichael [18] is that the observed signal allows us to generate an inferred quantum evolution conditioned on a particular observed record. In this way, the method works from the recorded signal to infer a quantum state evolution. In simulations, we have utilized this logic for computational convenience by using a random number generator to generate a “typical” sequence of observations. The assumption that we deal with an ensemble is appropriate for the case where several thousand ions are used, but it would be quite unsuitable for the description of an experiment performed on a single ion. Since such an experiment is likely to be made in the near future, it is important to attempt to describe the evolution of these individual realizations conditioned on the data acquired by the specific measurement scheme. For this reason we use the stochastic simulation methods that have been developed over the past few years for this purpose.

The motivation for the derivation of stochastic equations of motion for atomic states has come from two sources. The quantum jump approach of Dalibard, Castin, and Mølmer [12,13] (often referred to as the Monte Carlo wave-function method, or MCWF) was derived as a method for simulating processes, such as laser cooling, where the density-matrix method is unsuitable because of the storage limitations of calculating with very large density matrices (an equivalent approach was also derived at much the same time by Hegerfeldt and Wilser [14,15]). This method was also inspired by the observation and analysis of quantum jumps in single trapped ions [20–22]. The quantum state diffusion (QSD)

approach of Gisin and Percival [16], which is characterized by continuous small fluctuations to the quantum state rather than by discrete jumps, was driven by a theoretical desire to produce statistical forms of quantum mechanics. Wiseman and Milburn [17] and Carmichael [18] have linked these schemes by showing that they describe the evolution of quantum systems conditioned by the information gained through different kinds of measurement processes [19]. In both the QSD and MCWF methods, the evolution of the quantum state of a single subsystem embedded in a larger environment is governed by random processes. To reproduce the results of an ensemble of systems, as given by the density-matrix equations, the stochastic simulation is repeated many times and average properties are calculated. It has also recently been suggested that the probability distributions among the different states could be simulated directly in some cases by using Markov chains [23]. Since individual trajectories describe the evolution of single quantum systems, we have used them to investigate the behavior of a single ion in a quantum Zeno experiment.

The quantum jump method describes an evolution during a time step  $\delta t$  in which two possibilities may occur. Either a photon is emitted by the system and, in principle at least, detected by a photodetector, or it is not. If a photon is detected, then the state vector of the system (which represents our knowledge of the system) “jumps” to a lower level, usually the ground state. This is described by the action of a reservoir operator  $\hat{R}$  (also known as a Lindblad operator [24]), which for atomic systems is usually a lowering operator. For the Zeno system it is  $\hat{R} = \sqrt{\gamma}\sigma_{ca}^-$ , where  $\gamma$  is the rate of spontaneous emission from level  $|c\rangle$  and  $\sigma_{ca}^-$  is the lowering operator between the levels  $|c\rangle$  and  $|a\rangle$ ; hence, the state vector after a time  $\delta t$  in which a jump is recorded is given by

$$|\psi_{\text{jump}}(t + \delta t)\rangle = \mu \hat{R} |\psi(t)\rangle = |a\rangle, \quad (8)$$

where  $\mu$  is a normalization coefficient. The probability of a jump occurring in the interval  $\delta t$  is given by

$$\Delta P_{\text{jump}} = \langle \psi(t) | \hat{R}^\dagger \hat{R} | \psi(t) \rangle \delta t. \quad (9)$$

If no jump occurs, then the state vector evolves according to a non-Hermitian Hamiltonian:

$$H_{\text{eff}} = H - \left( \frac{i}{2} \hat{R}^\dagger \hat{R} \right), \quad (10)$$

$$|\psi_{\text{no-jump}}(t + \delta t)\rangle = \mu (1 - i \delta t H_{\text{eff}}) |\psi(t)\rangle, \quad (11)$$

where  $H$  is the isolated atom Hamiltonian.

The equations of motion for quantum state diffusion are governed by a stochastic Ito process. Within a time step  $\delta t$  the state evolves according to

$$|\delta\psi\rangle = -iH|\psi\rangle\delta t + \frac{1}{2}(2\langle\hat{R}^\dagger\rangle_\psi\hat{R} - \hat{R}^\dagger\hat{R} - \langle\hat{R}^\dagger\rangle_\psi\langle\hat{R}\rangle_\psi)|\psi\rangle\delta t + (\hat{R} - \langle\hat{R}\rangle_\psi)|\psi\rangle\delta\xi, \quad (12)$$

where  $H$  is the Hamiltonian describing the coherent evolution of the system, and  $\xi$  is a complex-valued random Wiener variable, which varies between each time step and each sample run, such that, when averaged,

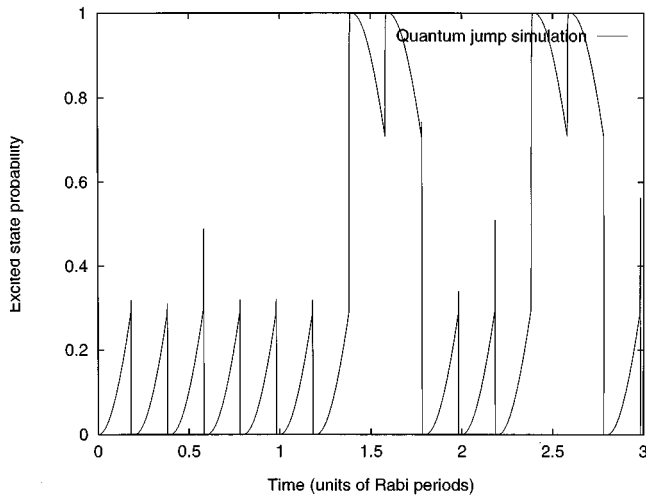


FIG. 4. A typical quantum trajectory calculated using the quantum jump method. The graph shows the probability of being in state  $|b\rangle$  as a function of time. The parameters are the same as in Fig. 3.

$$\overline{d\xi_t} = 0, \quad \overline{d\xi_t d\xi_{t'}} = 0, \quad \overline{d\xi_t^* d\xi_{t'}} = \delta_{t't}. \quad (13)$$

It has been shown that the evolution of a quantum system in this way can be derived from the assumption that the system is observed using a perfect heterodyne detector. In this case the state vector of the system is conditioned by the results measured by this kind of detector [17,19].

#### IV. APPLICATION OF STOCHASTIC METHODS TO THE QUANTUM ZENO EFFECT

The stochastic methods described in the preceding section were used to perform numerical simulations of the Zeno effect using the same parameters as were used in Sec. II for the density-matrix simulations. The computer programs were written in FORTRAN and run on Sun workstations.

A typical quantum trajectory produced using the quantum jump method is shown in Fig. 4. Outside of the measurement pulses, the state of the atom changes coherently between levels  $|a\rangle$  and  $|b\rangle$ . The effect of the measurement pulse is to change the state of the system in such a way that after the pulse the system is either in state  $|b\rangle$  or has jumped to state  $|a\rangle$  (after which the system undergoes interrupted fluorescence between  $|a\rangle$  and  $|c\rangle$  until the end of the measurement). If a quantum jump did occur, the state of the system returns rapidly to state  $|a\rangle$  after the measurement because this transition is heavily damped. The decision as to which of the two possible outcomes occurs is random. After the measurement pulse, the system returns to undergoing coherent evolution and the cycle repeats itself. Effectively what is seen by an observer using a photodetector are sequences of scattered light pulses separated by dark periods during which the measurement produces no fluorescence.

The quantum jump simulations were made many times, and the results were averaged (Fig. 5). It was found that the results approximated those of the density-matrix solution and that the discrepancy between the methods became increasingly small as the number of simulations was increased. In this way the quantum jump method reproduces the behavior when the quantum Zeno effect experiment is performed on

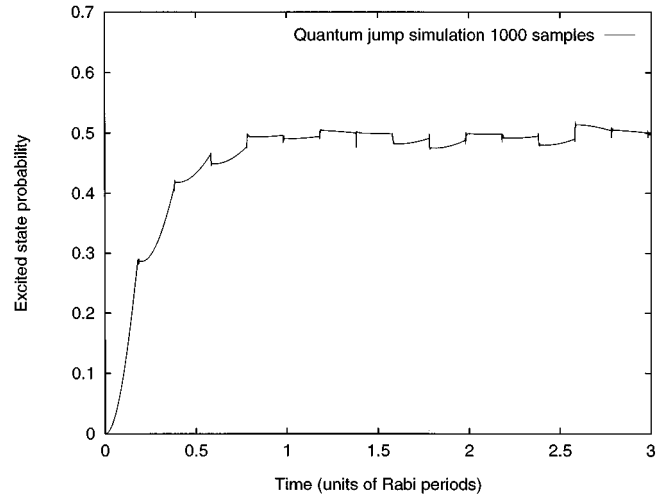


FIG. 5. The results of performing an ensemble average of 1000 quantum jump trajectories. As the number of samples increases, the results converge toward the density-matrix solution. The parameters are the same as in Fig. 3.

many ions simultaneously, and it also describes the results that would be expected if the single-ion experiment were performed many times and the results averaged.

A typical trajectory produced using the quantum state diffusion method is shown in Fig. 6. The overall behavior between the measurement pulses is the same as when the simulations are performed using the quantum jump method. The measurement pulse appears to have the same effect of transferring the system into either state  $|b\rangle$  or state  $|a\rangle$ . Again the decision between these possibilities is random, but the manner in which the state changes during the transition is different. The state appears to fluctuate rapidly during the measurement until it settles into one of the two possibilities. As the conditioned state vector represents our knowledge of the system, the results suggest that it is possible to deduce from

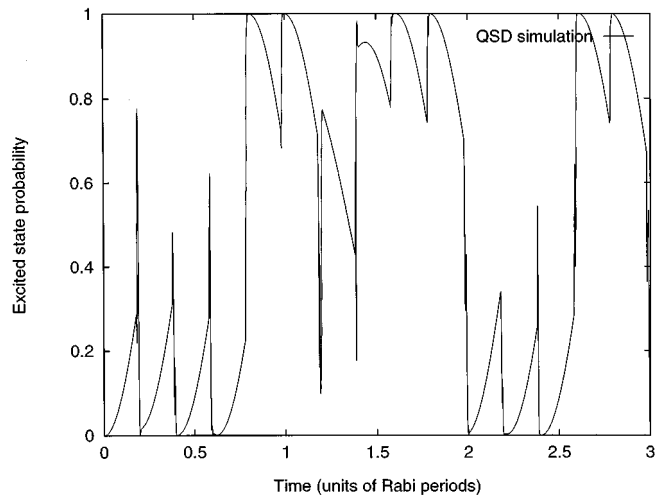


FIG. 6. A typical quantum trajectory calculated using the quantum state diffusion method. The graph shows the probability of being in state  $|b\rangle$  as a function of time. The parameters are the same as in Fig. 3. Notice that on one occasion the state of the system did not localize within the duration of the measurement pulse.

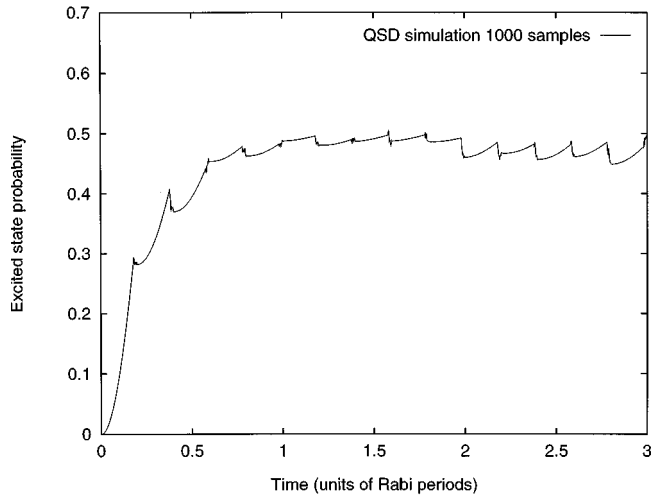


FIG. 7. The results of performing an ensemble average of 1000 trajectories calculated using the quantum state diffusion method. As with the ensemble of quantum jump simulations, the results converge to the density-matrix solutions as the number of samples increases. The parameters are the same as in Fig. 3.

the output of the heterodyne detector the final state of the atomic system after the measurement.

When an ensemble result is computed from the average of many such trajectories, the results of the quantum state diffusion simulations also converge to the density-matrix results (Fig. 7). The rate at which the results converge to the density-matrix solutions as a function of the number of trajectories sampled is approximately the same as with the quantum jump method [25].

## V. INTERPRETATION

Immediately before each measurement pulse the atomic system is in a superposition of two states  $|a\rangle$  and  $|b\rangle$ :

$$|\psi\rangle = c_a|a\rangle + c_b|b\rangle. \quad (14)$$

The measurement hypothesis states that the probability of being found in a particular state at the end of a measurement is given by the squared amplitude for the state at the beginning of the measurement. Consequently there should be a probability  $|c_a|^2$  that the system jumps to state  $|a\rangle$  and scatters photons, and a probability  $|c_b|^2$  that the system moves to state  $|b\rangle$  and no photons are scattered. To test this hypothesis for the measurement process in the Zeno experiment, samples of simulated quantum trajectories were made, starting from various initial superposition states. The samples were subjected to a single-measurement pulse, after which the fraction of trajectories found in each of the different states was recorded and plotted against the initial amplitude squared. If the measurement process were to conform with the measurement hypothesis, we would expect the graph produced to tend toward a straight line as the number of samples increases. The results of this analysis are shown in Fig. 8 for the quantum jump method, and Fig. 9 for the quantum state diffusion method. In addition the Markov chain method [23] was used to calculate the results of quantum jump simulations in the limit of very large sample sizes, as shown in Fig.

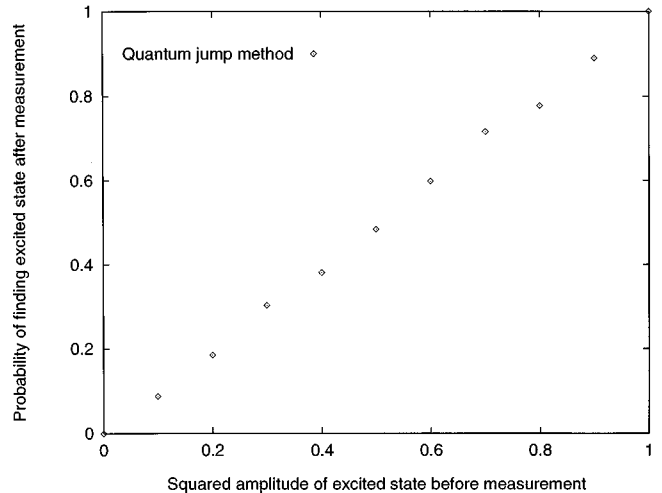


FIG. 8. A plot showing the probability of being in state  $|b\rangle$  at the end of a measurement as a function of the  $|b\rangle^2$  at the beginning of the measurement. The results were calculated by analyzing the results of 1000 quantum jump trajectories. The parameters are the same as in Fig. 3.

10. The results clearly show that for the parameters chosen the measurement process does conform reasonably well to the measurement hypothesis.

In Fig. 11 a small region of the time evolution of a quantum jump trajectory is enlarged to show the important features. Until the start of the measurement, the trajectory follows the deterministic trajectory for an undamped driven two-level system. At the start of the measurement pulse, the state of the system follows a “no-jump trajectory,” which rapidly converges toward state  $|b\rangle$ , which is an eigenstate of the no-jump evolution [26,27]. However, while this is happening there is always a probability that the state of the system will jump down to the lower level. If this does not occur,

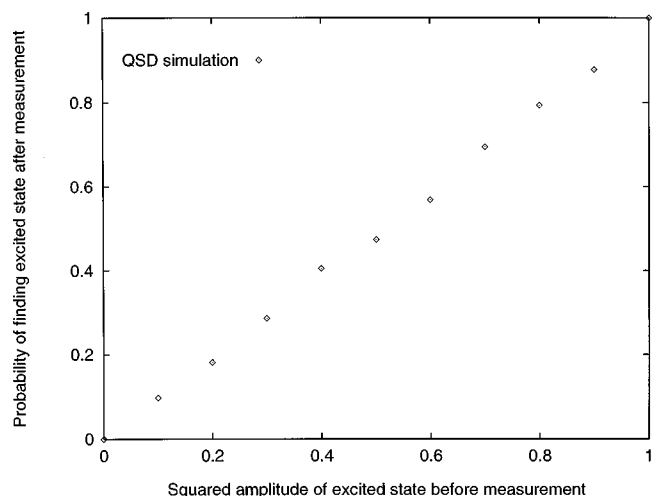


FIG. 9. The probability of being in state  $|b\rangle$  at the end of a measurement as a function of  $|b\rangle^2$  at the beginning of the measurement. The results were calculated by analyzing the results of 1000 quantum state diffusion trajectories. For the QSD simulations the final state is considered for the sake of definiteness to be in state  $|b\rangle$  if its projection onto  $|b\rangle$  is greater than 90% (i.e.,  $|\langle\psi|b\rangle|^2 > 0.9$ ).

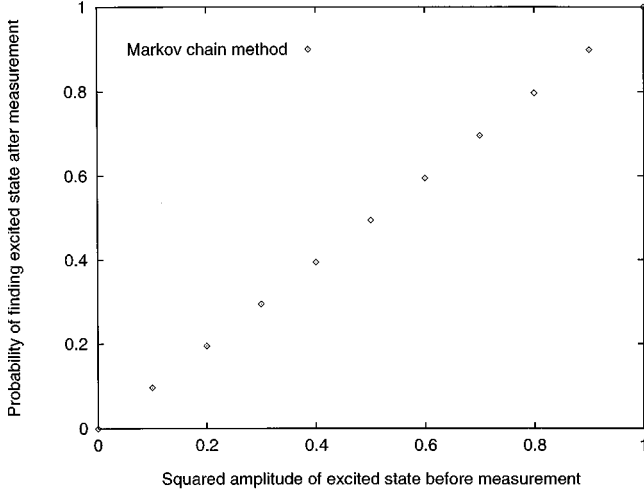


FIG. 10. The probability of being in state  $|b\rangle$  at the end of a measurement as a function of  $|b|^2$  at the beginning of the measurement. The results were calculated using the Markov chain method, which produces the same results as a very large sample of quantum jump trajectories

then the state will arrive in the excited state. If a jump does occur, as shown in the example, then once the atom has jumped to state  $|a\rangle$  it then undergoes repeated jumps between levels  $|c\rangle$  and  $|a\rangle$ . This means there is a sequence of photons scattered from this transition, which occurs until the end of the measurement pulse. The no-jump trajectory can be evaluated analytically by solving for the motion with the effective Hamiltonian [26,27], making the assumption that the rf field is negligible during the measurement pulse and

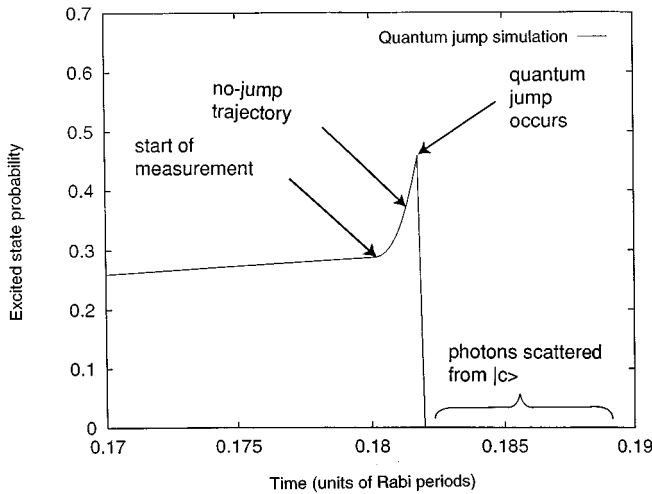


FIG. 11. Magnified section of a quantum jump trajectory during the measurement pulse. The probability of occupying state  $|b\rangle$  is shown as a function of time. Until the start of the measurement, the occupation probability rises slowly because of the radio-frequency driving. During the measurement the probability rises sharply toward 1. However, in this example, a quantum jump occurs and the state of the system jumps to the ground state. After this occurs, the atom undergoes interrupted Rabi oscillations between  $|a\rangle$  and  $|c\rangle$ . During this process many photons are scattered from the system, which are detected by the measurement apparatus.

then calculating the normalization coefficients. At the start of the measurement pulse,

$$|\psi(t=0)\rangle = c_a(0)|a\rangle + c_b(0)|b\rangle. \quad (15)$$

The effective Hamiltonian is

$$H_{\text{eff}} = \frac{\Omega}{2} (\sigma_{ac}^+ + \sigma_{ac}^-) - i \frac{\gamma}{2} \sigma_{ac}^+ \sigma_{ac}^-. \quad (16)$$

This produces the following differential equations for the coefficients of  $|\psi(t)\rangle = c_a(t)|a\rangle + c_b(t)|b\rangle + c_c(t)|c\rangle$ :

$$\dot{c}_a = -i \frac{\Omega}{2} c_b(t), \quad (17)$$

$$\dot{c}_b = -i \frac{\Omega}{2} c_a(t), \quad (18)$$

$$\dot{c}_c = 0. \quad (19)$$

This neglects the renormalization after each step, but this can be left until after the solutions have been found since the equations are linear. In the unsaturated case  $\gamma > 2\Omega$ ,

$$c_a(t) = c_a(0) e^{-\gamma t/4} \left( \cosh \lambda t + \frac{\gamma}{4\lambda} \sinh \lambda t \right), \quad (20)$$

$$c_b(t) = \frac{c_a(0) i \Omega}{2\lambda} e^{-\gamma t/4} \sinh \lambda t, \quad (21)$$

$$c_c(t) = c_c(0), \quad (22)$$

where  $\lambda = (\gamma^2 - 4\Omega^2)^{1/2}/4$ . The coefficients can then be normalized:

$$\bar{c}_a(t) = \frac{c_a(t)}{\sqrt{|c_a(t)|^2 + |c_b(t)|^2 + |c_c(t)|^2}}, \quad (23)$$

$$\bar{c}_b(t) = \frac{c_b(t)}{\sqrt{|c_a(t)|^2 + |c_b(t)|^2 + |c_c(t)|^2}}, \quad (24)$$

$$\bar{c}_c(t) = \frac{c_c(t)}{\sqrt{|c_a(t)|^2 + |c_b(t)|^2 + |c_c(t)|^2}}. \quad (25)$$

A comparison of numerical calculations and the formulas given by Eqs. (20)–(25) is shown in Fig. 12.

The fluorescence from a single ion in the quantum Zeno effect experiment is such that in any individual measurement pulse the ion may or may not emit photons (Fig. 4). The probability of emitting photons at a particular measurement depends on whether or not the ion had emitted a photon at the time of the previous measurement. This process can be described as a simple Markov chain [28]. Let  $M_n = 1$  represent the event that photons are detected during the  $n$ th measurement pulse and  $M_n = 0$  if they are not; then,

$$Pr(M_n = 1 | M_{n-1} = 1) = \alpha, \quad (26)$$

$$Pr(M_n = 0 | M_{n-1} = 1) = 1 - \alpha, \quad (27)$$

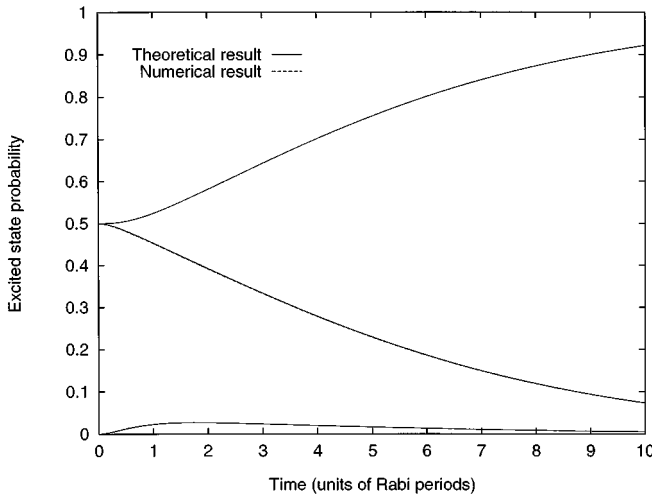


FIG. 12. Comparison of the no-jump trajectories calculated analytically in Eqs. (15)–(25) and the result of a numerical calculation. The parameters chosen were  $\Omega_2=1$  and  $\gamma=4$ . The agreement is sufficiently good that the results are hard to distinguish.

$$Pr(M_n = 1 | M_{n-1} = 0) = \beta, \quad (28)$$

$$Pr(M_n = 0 | M_{n-1} = 0) = 1 - \beta. \quad (29)$$

In the case considered here, where there is no detuning or damping of the  $|a\rangle$ - $|b\rangle$  transition,

$$\alpha = \beta = \cos^2 \frac{\Omega_1 t}{2}. \quad (30)$$

This behavior of jumping between two possible outcomes according to fixed transition probabilities is closely analogous to the behavior of a trapped ion in a quantum jump experiment. It is only when several ions are present in the experiment simultaneously that the signal of the fluorescence

becomes proportional to the populations predicted by the density matrix; this is because, for a large number of ions, the fraction of ions in a given state at any particular time converges toward the probability that an individual ion may be found in that state [23,25].

In the proposed single-ion experiment it is unclear whether or not it will be possible to detect the fluorescence from each individual measurement pulse. If it were possible, then the result predicted by the quantum jump method would be the observation of sequences of a random number of light pulses, interspersed with periods in which no photons were visible. In practice, optical pumping effects limit the number of photons that can be scattered during a single measurement, and this effect, combined with a limited detector efficiency, makes the detection of individual pulses difficult. Approximate calculations suggest that this behavior is at the limit of what it may be experimentally possible to observe.

## VI. CONCLUSIONS

The quantum trajectories produced by stochastic simulations of the Zeno effect show the correct probabilistic results to conform to the measurement hypothesis, and they also reproduce the density-matrix probabilities for an ensemble of particles. The measurement process could be regarded as a dynamical process during which the wave function collapses. The nature of this collapse differs according to the different simulation schemes. For the quantum jump technique it is possible to calculate some analytical properties of this process, but this appears to be very difficult for the quantum state diffusion process [29].

## ACKNOWLEDGMENTS

We would like to thank Richard Thompson, Daniel Segal, and Barry Garraway for helpful discussions. This work was supported in part by the U.K. Engineering and Physical Sciences Research Council and by the European Union.

- 
- [1] B. Misra and E. C. G. Sudarshan, *J. Math. Phys.* **18**, 756 (1977).  
 [2] A. Peres, *Am. J. Phys.* **48**, 931 (1980).  
 [3] G. J. Milburn, *J. Opt. Soc. Am. B* **5**, 1317 (1988).  
 [4] M. J. Gagen, H. M. Wiseman, and G. J. Milburn, *Phys. Rev. A* **48**, 132 (1993).  
 [5] J. I. Cirac, A. Schenzle, and P. Zoller, *Europhys. Lett.* **27**, 123 (1994).  
 [6] R. Cook, *Phys. Scr.* **T21**, 49 (1988).  
 [7] W. M. Itano, D. J. Heinzen, J. J. Bollinger, and D. J. Wineland, *Phys. Rev. A* **41**, 2295 (1990).  
 [8] V. Frerichs and A. Schenzle, *Phys. Rev. A* **44**, 1962 (1991).  
 [9] E. Block and P. R. Berman, *Phys. Rev. A* **44**, 1466 (1991).  
 [10] R. C. Thompson and D. M. Segal (private communication).  
 [11] J. von Neumann, *Mathematische Grundlagen der Quantentheorie* (Springer, Berlin, 1931) [English translation: *Mathematical Foundations of Quantum Mechanics* (Princeton University Press, Princeton, NJ, 1955)].  
 [12] J. Dalibard, Y. Castin, and K. Mølmer, *Phys. Rev. Lett.* **68**, 580 (1992).  
 [13] K. Mølmer, Y. Castin, and J. Dalibard, *J. Opt. Soc. Am. B* **10**, 524 (1993).  
 [14] G. C. Hegerfeldt and T. S. Wilser, in *Proceedings of the II International Wigner Conference, Gaslar, 1991*, edited by H. D. Doebner *et al.* (World Scientific, Singapore, 1991).  
 [15] G. C. Hegerfeldt *Phys. Rev. A* **47**, 449 (1993).  
 [16] N. Gisin and I. C. Percival, *J. Phys. A* **25**, 5677 (1992).  
 [17] H. M. Wiseman and G. J. Milburn, *Phys. Rev. A* **47**, 1652 (1993).  
 [18] H. J. Carmichael, *An Open Systems Approach to Quantum Optics*, Lecture Notes in Physics (Springer-Verlag, Berlin, 1994).  
 [19] P. L. Knight and B. M. Garraway, in *Proceedings of the 44th*

- Scottish Universities Summer School in Physics*, edited by G-L. Oppo *et al.* (IOP, Bristol, 1995).
- [20] S. Reynaud, J. Dalibard, and C. Cohen-Tannoudji, *IEEE J. Quantum Electron.* **24**, 1395 (1988).
- [21] C. W. Gardiner, A. S. Parkins, and P. Zoller, *Phys. Rev. A* **46**, 4363 (1992).
- [22] M. S. Kim and P. L. Knight, *Phys. Rev. A* **40**, 5265 (1987); **40**, 215 (1989).
- [23] W. L. Power, *J. Mod. Opt.* **42**, 913 (1995).
- [24] G. Lindblad, *Commun. Math. Phys.* **48**, 119 (1976).
- [25] J. Steinbach, B. M. Garraway, and P. L. Knight, *Phys. Rev. A* **51**, 3302 (1995).
- [26] J. Steinbach, International Diploma of Imperial College thesis, 1994 (unpublished).
- [27] J. Steinbach, B. M. Garraway, and P. L. Knight, *Acta Phys. Slovaca* **45**, 289 (1995).
- [28] Y. A. Rozanov, *Probability Theory: A Concise Course* (Dover, New York, 1977).
- [29] P. Goetsch and R. Graham, *Phys. Rev. A* **51**, 136 (1995).